Supporting Information

Octamolybdate-based Hybrid Constructed by Flexible Bis-triazole Ligands: Synthesis, Photocatalytic and Electrochemical Properties

Jiaqi Chi, Mingyue Fan, Zhongmin Su*, Xiao Li*, Jing Sun, Chen Zhou, Xiaoli Hu

School of Chemistry and Environmental Engineering, Changchun University of Science and Technology, Changchun, 130022 (China)
Jilin Provincial Science and Technology Innovation Center of Optical Materials and Chemistry, Changchun, 130022, China
Corresponding author
E-mail addresses: zmsu@nenu.edu.cn (Z. Su); lix@cust.edu.cn (X. Li)

1. Experimental

1.1. Materials and general methods

The reagents and solvents used in the experiment were purchased from commercial sources and used without further purification. The selected ligand btrp was synthesized according to the reported literature [1]. The diffraction data of crystal cell of **1** were collected by Bruker APEX II CCD diffractometer. Infrared spectra of solid samples were acquired from a Nicolet Magna750 FTIR spectrometer in the 400-4000 cm^{-1} region with a KBr pellet. PXRD patterns were carried by a DRIC Y-2000 X-ray diffractometer with CuKα (λ = 1.5418 Å) radiation in the range of 5-50°at 293K. Thermogravimetric analysis (TGA) was executed on an EVO2G-TG-08 analyzer heated from room temperature to 800 °C under nitrogen atmosphere at a rate of 10 °C min^{-1}. UV-Vis absorption spectra were inspected on a UV-5500 (PC) in the range of 200-800 nm. The visible light source in the photocatalytic dye degradation experiment was provided by CEL-HXF300 produced by Beijing Zhongjiao Jinyuan Technology Co. LTD Electrochemical testing and data were examined on CHI 760E electrochemical workstation. The three-electrode system was used with an Ag/AgCl electrode as the reference electrode and a graphite carbon rod as the counter electrode. The compound modified as carbon paste electrodes (CPE) served as the working electrodes.

1.2 Synthesis of [Co(btrp)$_2$(H$_2$O)$_2$(β-Mo$_8$O$_{26}$)$_{0.5}$]·H$_2$O (1).

A mixture of Co(NO$_3$) ·6H$_2$O (0.10 g, 0.34 mmol), Na$_2$MoO$_4$·2H$_2$O (0.10 g, 0.08 mmol) and btrp (0.03 g, 0.17 mmol) (Scheme S1) were dissolved in 10 mL of deionized water. The solution was ultrasonic agitated for 30 min at room temperature, and a few drops of HNO$_3$ was added to the solution, Then the solution was sealed in a 25 mL Teflon-lined autoclave at 140 °C for 3 days. After

cooling to room temperature, Red block crystals were formed. Yield about 62% based on Mo. Anal. Calcd for **1** (%): C, 15.83; H, 2.45; O, 24.12; N, 15.83; Co, 5.56; Mo, 36.19. Found: C, 15.78; H, 2.44; O, 24.19; N, 15.78; Co, 5.58; Mo, 36.30.

1.3. Preparation of 1 bulk-modified CPE.

The complexes bulk-modified CPE was fabricated as follows: 0.20 g graphite powder and 20 mg complexes were mixed and ground with an agate mortar and pestle for approximately 30 min to achieve a uniform mixture, then 0.10 mL of para□n oil was added and stirred with a copper rod. The homogenized mixture was placed in a 3mm inner diameter glass tube and the tube surface was wiped by weighing paper. The electrical contact was established through the copper rod on the back of the electrode.

1.4. X-ray crystallographic study.

Single-crystal X-ray diffraction data for **1** was recorded on a Bruker Apex II CCD diffractometer with graphite monochromator using Mo-Kα radiation (λ = 0.71073 Å) at 273 K. Absorption corrections were applied using the multi-scan technique. The structure was solved by the direct methods of SHELXT and refined by the full-matrix least-squares technique with the SHELXL program [2]. Non-hydrogen atoms were refined with anisotropic temperature parameters. In **1**, the Mo_8 core exists disorder phenomenon. The disordered atoms O16 and O8, O24 and O12, O14 and O17, O15 and O22, O10 and O18, O11 and O19, O13 and O23, Mo3 and Mo8, Mo5 and Mo6, Mo4 and Mo7 were disordered over two sites with occupancy of 0.85 and 0.15 and were anisotropically refined. In the ligand of btrp, carbon atoms (C8 and C18, C11 and C19, C13 and C16, C14 and C15 and C12 and C17) and three nitrogen atoms (N11 and N2, N15 and N14 and N3 and N13) were disordered over two sites with occupancy of 0.8 and 0.2, which were anisotropically refined. The crystal data and structure refinement results of **1** is summarized in Table S1. The CCDC number of **1** is 1972437.

1.5. Process of photocatalysis.

10 mg of the compound was suspended in 20 mL 10 mg/L dyes aqueous solution, respectively. The suspension was stirred in the dark for one hour to achieve adsorption-desorption equilibrium. Under agitation, the suspension was exposed to the light source. At regular intervals, a small amount of sample solution was centrifuged and the absorbance was measured with an ultraviolet spectrophotometer. The control experiment and rate constant curves were shown as Figure S6 - Figure S11. And the repetitive experiments were also shown in Figure S12 and S13.

Reference:

[1] EY Semitut, TS Sukhikh, EY Filatov, GA Anosova, AA Ryadun, KA Kovalenko and AS Potapov. Synthesis, Crystal Structure, and Luminescent Properties of Novel Zinc Metal–Organic Frameworks Based on 1,3-Bis(1,2,4-

triazol-1-yl)propane. Cryst Growth Des 2017; 17: 5559-5567. https://doi.org/10.1021/acs.cgd.7b01133.

[2] GM Sheldrick, A short history of SHELX. Acta Crystallogr Sect A: Found Crystallogr 2008; 64: 112-122. https://doi.org/10.1107/S0108767307043930.

Table S1. Crystallographic Data for 1.

Empirical formula	$C_{14}H_{26}CoMo_4N_{12}O_{16}$
Formula weight	1061.16
Temperature/K	273.15
Crystal system	monoclinic
Space group	$P2_1/n$
a/Å	11.734(2)
b/Å	21.779(4)
c/Å	12.503(2)
α/°	90
β/°	104.189 (2)
γ/°	90
Volume/Å^3	3097.6(9)
Z	4
density (calculated)	2.275 g/cm^3
absorption coefficient	2.188 mm^{-1}
F(000)	2068.0
Crystal size/mm^3	0.24 × 0.22 × 0.2
2Θ range for data collection/°	3.74 to 56.596
Index ranges	-15 ≤ h ≤ 14, -23 ≤ k ≤ 29, -14 ≤ l ≤ 16
Reflections collected	22832
Independent reflections	7681 [R_{int} = 0.0281, R_{sigma} = 0.0319]
Data/restraints/parameters	7681/77/605
Goodness-of-fit on F^2	1.052
R_1 [I>=2σ (I)] [a]	0.0239
wR_2[I>=2σ (I)] [b]	0.0536
R_1 [all data] [a]	0.0302
wR_2[all data] [b]	0.0563
Largest diff. peak/hole / e Å^{-3}	0.47/-0.65

[a]$R1 = \sum||F_0| - |F_c||/\sum|F_0|$. [b]$wR_2 = [\sum w(F_0^2 - F_c^2)^2/\sum w(F_0^2)^2]^{1/2}$

Table S2. Selected Bonds Lengths (Å) for 1.

Co1-O4	2.1541(19)	Co1-N3	2.109(4)
Co1-O8	2.14(4)	Co1-N6[3]	2.170(2)
Co1-N1[2]	2.131(2)	Co1-O16	2.079(6)
Co1-N2	2.106(2)	Co1-N13	2.132(10)

[1]2-X,-Y,-Z; [2]1+X,+Y,+Z; [3]+X,+Y,-1+Z

Table S3. Selected Bonds Angles (°) for 1.

O4-Co1-N6[2]	89.85(8)	N2-Co1-N13	87.3(6)
O8-Co1-O4	173.2(8)	N3-Co1-O4	89.57(18)
N1[3]-Co1-O4	86.86(8)	N3-Co1-N1[3]	93.36(19)
N1[3]-Co1-O8	98.8(8)	N3-Co1-N6[2]	178.9(2)
N1[3]-Co1-N6[2]	87.51(8)	O16-Co1-O4	176.80(18)
N1[3]-Co1-N13	96.8(6)	O16-Co1-N1[3]	90.59(18)
N2-Co1-O4	90.02(8)	O16-Co1-N2	92.66(18)
N2-Co1-O8	84.6(8)	O16-Co1-N3	88.7(2)
N2-Co1-N1[3]	174.98(9)	O16-Co1-N6[2]	91.96(17)
N2-Co1-N3	90.55(19)	N13-Co1-O4	92.0(5)
N2-Co1-N6[2]	88.55(8)	N13-Co1-O8	83.5(11)

[1]2-X,-Y,-Z; [2]+X,+Y,-1+Z; [3]1+X,+Y,+Z; [4]-1+X,+Y,+Z; [5]+X,+Y,1+Z
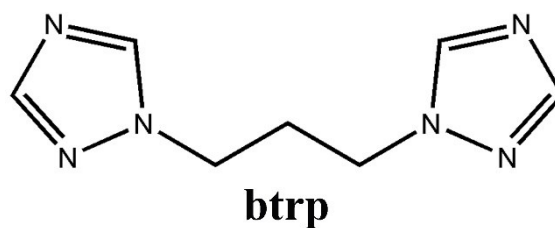
btrp

Scheme S1. The ligands 1,3-bis(1,2,4-triazol-1-yl) propane (btrp).
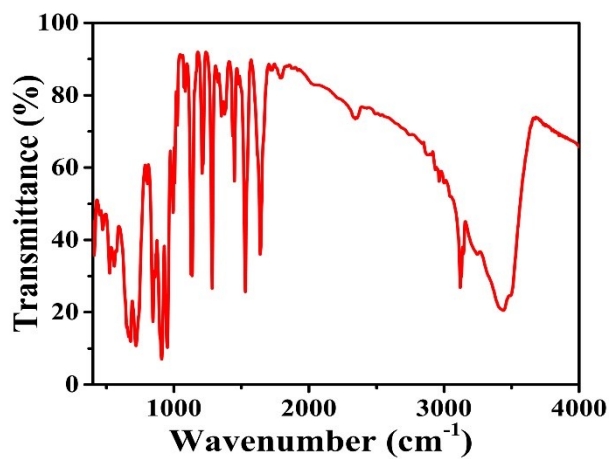
Figure S1. The IR spectra of **1**.
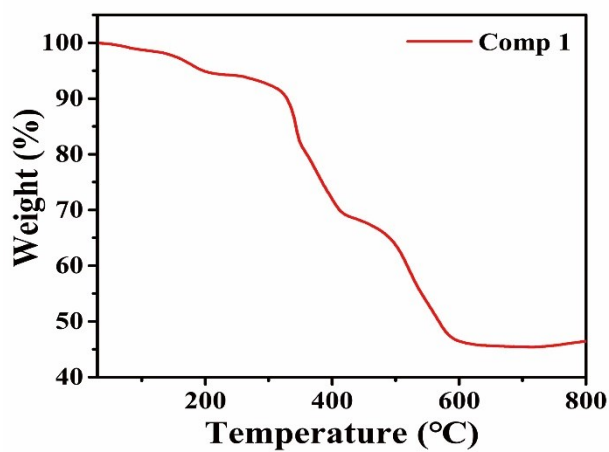
Figure S2. The TGA curves of **1**.
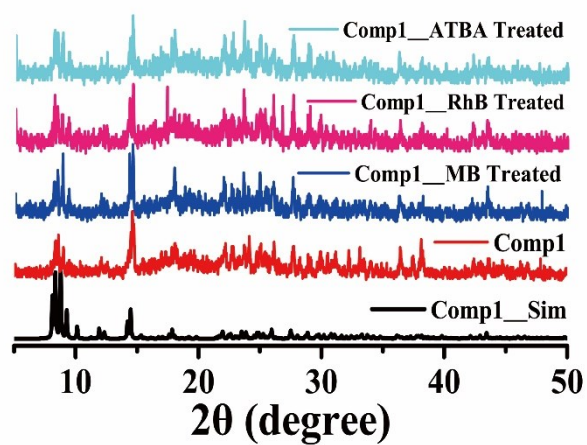
Figure S3. The PXRD patterns of **1** simulated (black), experimental (red) and after photocatalysis.
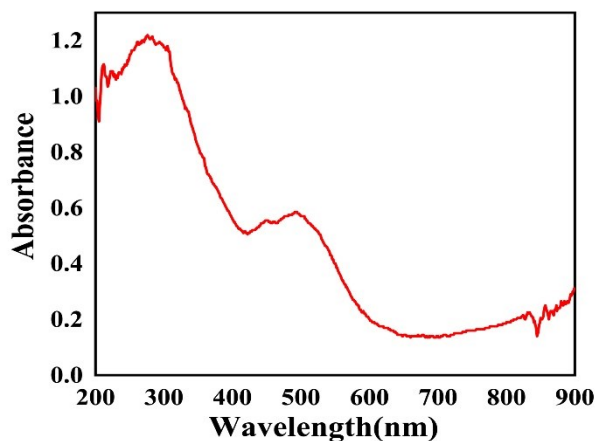
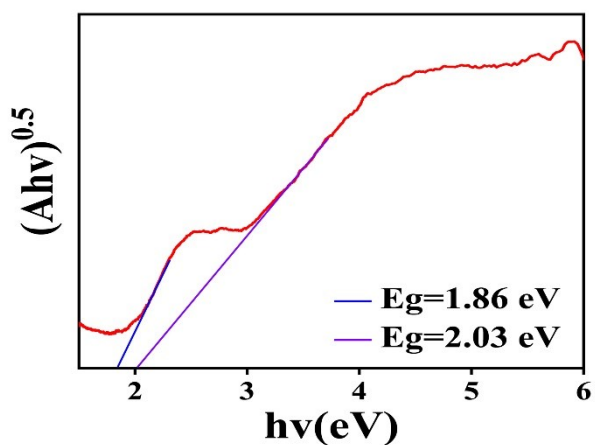Figure S4. The diffuse reflection spectra of **1** in the crystalline state.

Figure S5. the plots of $(\alpha h v)^{0.5}$ vs photon energy (hv) of **1**.

To evaluate the semiconductor performance and photocatalysis activitie of **1**, the diffuse reflection spectra of **1** was carried out in the crystalline state at room temperature. According to the UV-vis DSR spectrum, the band gap width was calculated by using the Tauc plot method

$$(\alpha h v)^{0.5}=A(h v-E_g)$$

In the formula: α is absorption coefficient, h is Planck's constant, v is the frequency of the light, A is constant, E_g is semiconductor forbidden band width. According to the above formula, the bandgap width of the crystal is calculated to be 1.84 eV and 2.01 eV. The band gap values indicate that **1** may respond to visible light irradiation and has the potential capacity for photocatalytic reactions.
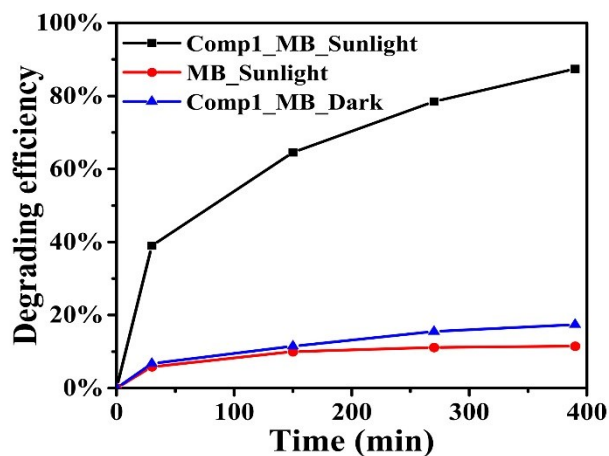
Figure S6. The degrading efficiency curve of MB solution under different conditions.
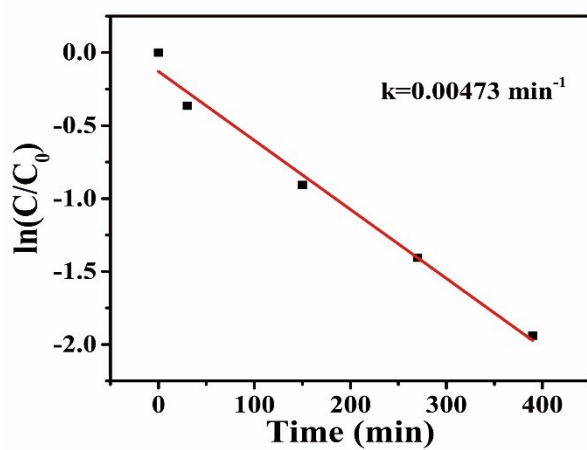
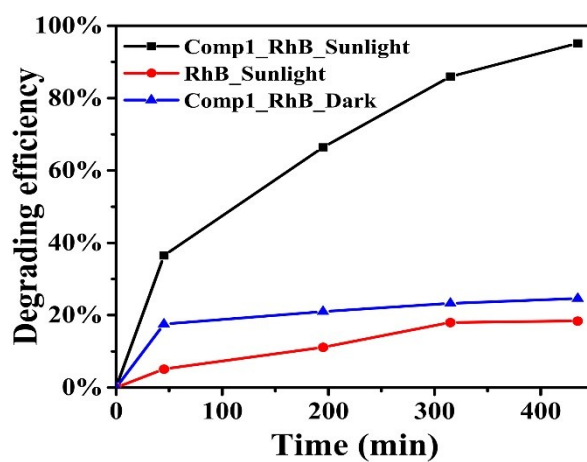Figure S7. The rate constant curve of photocatalytic degradation of MB by **1**.

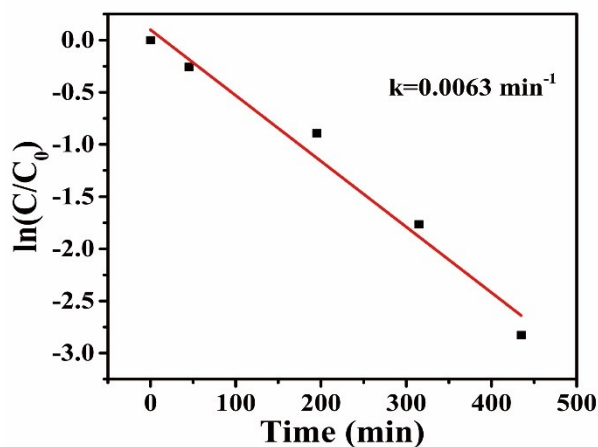Figure S8. The degrading efficiency curve of RhB solution under different conditions.

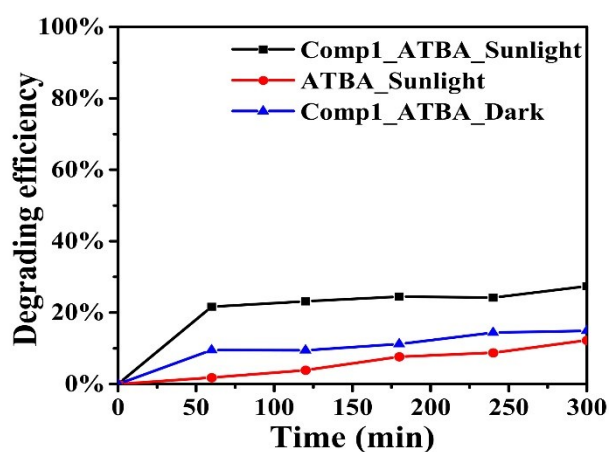Figure S9. The rate constant curve of photocatalytic degradation of RhB by **1**.

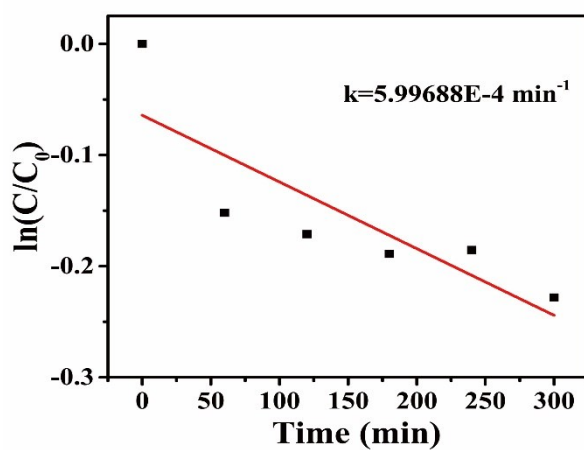Figure S10. The degrading efficiency curve of ATBA solution under different conditions.

Figure S11. The rate constant curve of photocatalytic degradation of ATBA by **1**.

The absorbance of dyes of the photo degradation processes without catalysts and the dark degradation processes with catalysts were compared. By comparison, the absorbance of the dyes without catalyst and without light hardly changed. While, the absorbance of Methylene blue (MB)

and Rhodamine B (RhB) dye solutions decreased with time when the catalyst was added and the light was irradiated. The absorbance of AlphazurineA (ATBA) barely changed. This indicates that **1** has photocatalytic with selectivity activity.
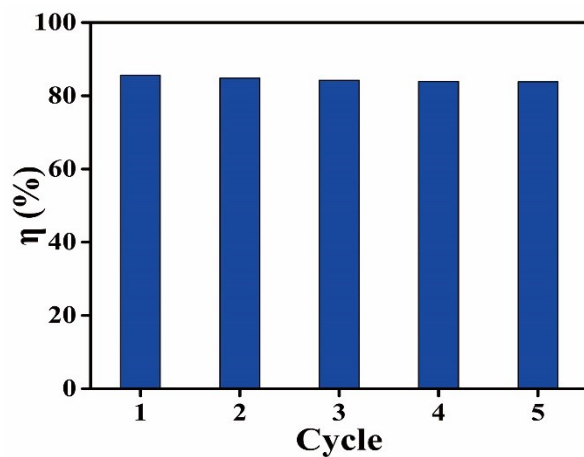

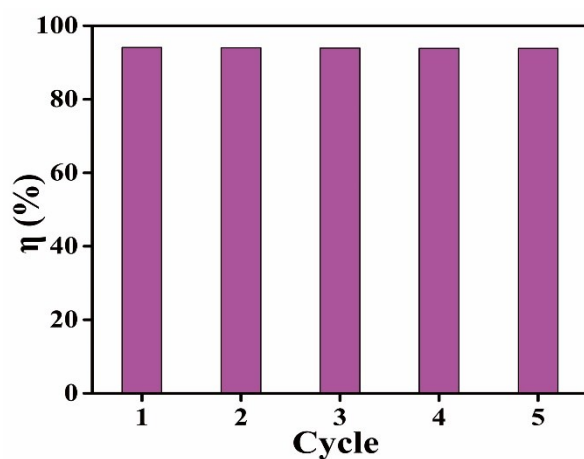Figure S12. MB degradation efficiency of **1** across 5 cycles.

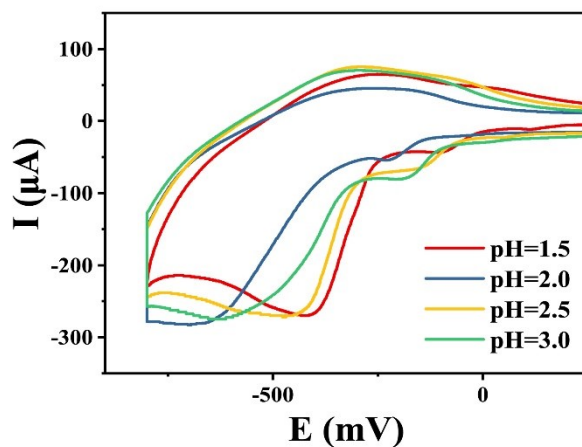Figure S13. RhB degradation efficiency of **1** across 5 cycles.

Figure S14. CVs of Mo_8-CPE in H_2SO_4 + Na_2SO_4 solutions at different pH. Scan rate: 250 mV s^{-1}.
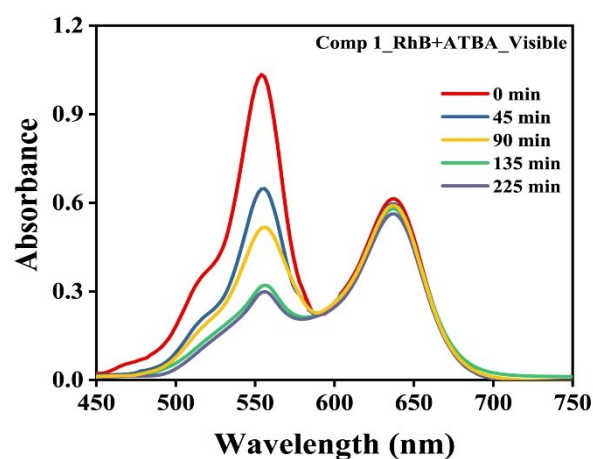
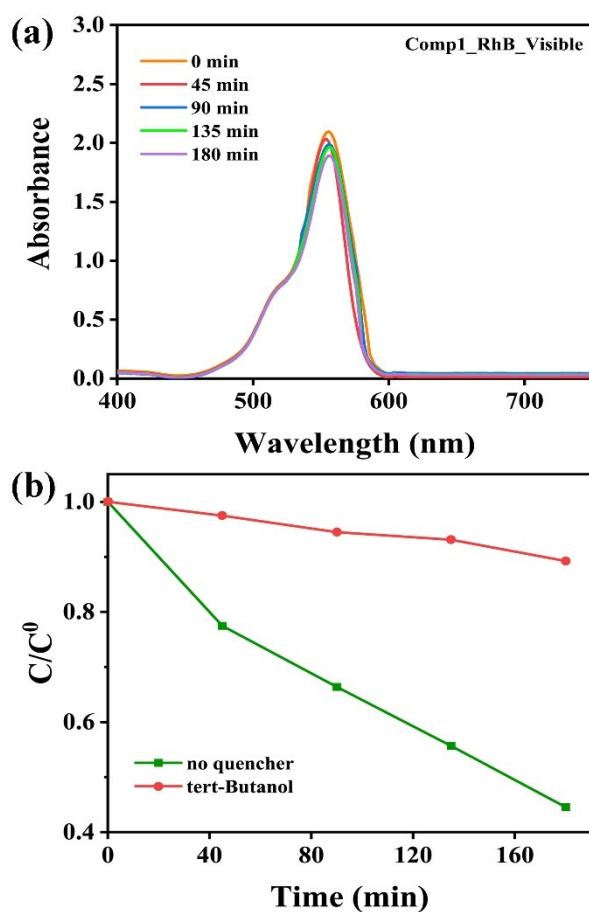Figure S15. Absorption spectra of the RhB + ATBA solution under light irradiation in the presence of **1**.

Figure S16. (a) Time dependent UV-Vis spectra of aqueous dyes under light irradiation in the present of **1** and tert-Butanol and (b) dynamic curves of aqueous dyes degradation.
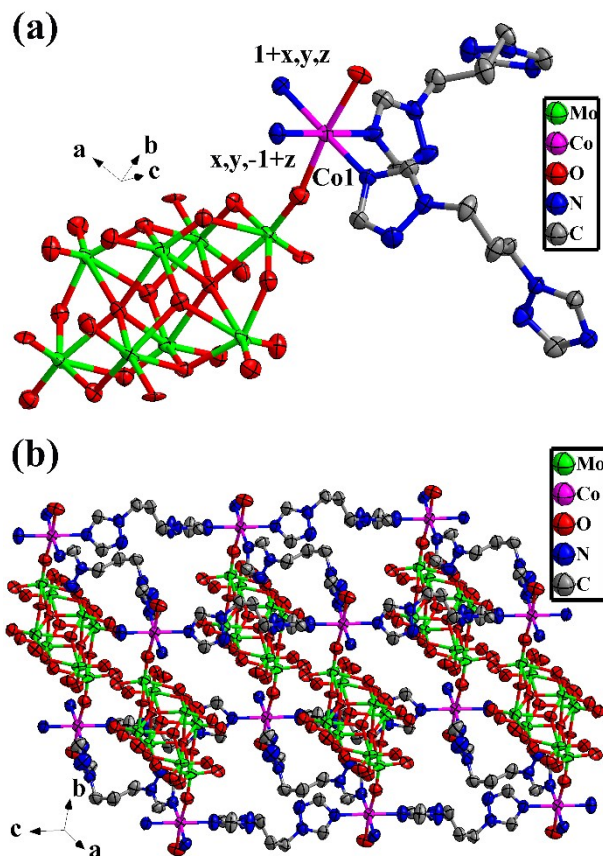
Figure S17. (a) The ellipse model of skew symmetric unit cell of the connected core of 1. The H atoms are dislodged. (b) The diagram of the 2D fabric of the connected core of 1.

In another of the connections, Mo_8 core is connected directly to the Co1. Co1 equips six-coordinated octahedral geometrical configuration. It was beset by bound water, POMs' oxygen atom and four nitrogen atoms which is derived from btrp ligands (Figure S17a). In **1**, btrp ligands chelate Co atoms through N donors to build layer. Furthermore, In the middle of the ligand layers, $[\beta-Mo_8O_{26}]$ anions combine with Co through oxygen to construct a 2D structure (Figure S17b).